AAPT PHYSICS EDUCATION | AMERICAN JOURNAL of PHYSICS

# Revisiting the Bragg reflector to illustrate modern developments in optics

S. A. R. Horsley, J.-H. Wu, M. Artoni, and G. C. La Rocca

Citation: American Journal of Physics **82**, 206 (2014); doi: 10.1119/1.4832436

View online: http://dx.doi.org/10.1119/1.4832436

View Table of Contents: http://scitation.aip.org/content/aapt/journal/ajp/82/3?ver=pdfcov

Published by the American Association of Physics Teachers





# Revisiting the Bragg reflector to illustrate modern developments in optics

S. A. R. Horsley[a)]
*Electromagnetic and Acoustic Materials Group, Department of Physics and Astronomy, University of Exeter, Stocker Road, Exeter EX4 4QL, United Kingdom*

J.-H. Wu
*College of Physics, Jilin University, Changchun 130012, People's Republic of China*

M. Artoni
*European Laboratory for Nonlinear Spectroscopy, Sesto Fiorentino, Italy and Department of Engineering and Information Technology, CNR-IDASC Sensor Laboratory, Brescia University, Brescia, Italy*

G. C. La Rocca
*Scuola Normale Superiore and CNISM, Pisa, Italy*

(Received 21 January 2013; accepted 6 November 2013)

A series of thin layers of alternating refractive index are known to make a good optical mirror over certain bands of frequency. Such a device, often termed the *Bragg reflector*, is usually introduced to students in isolation from other parts of the curriculum. Here, we show that the basic physics of wave propagation through a stratified medium can be used to illustrate some more modern developments in optics and quantum physics, from transfer matrix techniques to the optical properties of cold trapped atoms and optomechanical cooling. We also show a simple example of how such systems exhibit an appreciable level of optical nonreciprocity. 
[http://dx.doi.org/10.1119/1.4832436]

## I. INTRODUCTION

To paraphrase Griffiths,[1] wave motion can be divided into at least three types: traveling waves (continuous spectrum), bound states (discrete spectrum), and waves within a periodic medium (continuous spectrum with forbidden regions). There are a variety of ways in which the third of these can be introduced, perhaps the most obvious of which is through condensed matter physics, where the atomic lattice provides an example of a periodic medium.[2–4]

In the context of condensed matter then, it is instructive to observe the emergence of Bloch's theorem as the number of periods of the system is increased. The motion of waves in a one-dimensional periodic, layered medium can be treated analytically for any number of layers.[1,5–7] An example where the onset of a band gap may be observed can be found in the optics of the Bragg reflector,[5] which is an optical medium composed of layers of two kinds of material with differing refractive indices. A compelling lesson one learns through studying an arbitrary number of layers is how quickly the results of Bloch's theorem become applicable as the number of layers is increased from unity. However, this is not usually the reason for introducing the Bragg reflector to students. It is often introduced as an optical component in an appropriate course, and more completely in a specialized course covering photonic crystals or microcavities. We find the Bragg reflector not only useful for discussing the emergence of Bloch's theorem, but it also reveals some subtleties of propagation in a periodic medium. Dispersion and dissipation alter the picture, and dissipation in particular can cause a breakdown of the distinction between allowed and forbidden bands.

Here, we briefly derive the optical properties of the Bragg reflector through an application of the transfer matrix formalism.[8] The results are then applied to the discussion of the optical properties of a lattice of cold trapped atoms,[9] where both dispersion and dissipation are significant at the frequencies of interest. As we shall see, the picture becomes quite different when these effects are included. Further, we show that the Bragg reflector can be used to introduce the principles of two phenomena of current interest: optomechanical cooling[10] and optical nonreciprocity.[11,12] In both cases, the high-frequency sensitivity close to a band edge couples the optical response to the center-of-mass motion of the reflector, thereby providing a simple example system where such effects can be exactly described.

## II. STRATIFIED MEDIA AND TRANSFER MATRICES

The problem of solving the wave equation in a medium that is inhomogeneous in only one direction can be reduced to the problem of multiplying $2 \times 2$ matrices together. This is known as the *transfer matrix* technique.[5,8] The technique is introduced here, but for a more in-depth exposition see the recent paper by Sánchez–Soto *et al.*[8] or the book by Yeh.[13]

A typical stratified system is shown in Fig. 1, where we have a medium composed of $N$ layers, each with a different value of the refractive index $n$, immersed in a background medium (perhaps a fluid) with index $n_c$. In general, the refractive indices of the layers will be complex numbers, the imaginary parts of which indicate the degree to which the electromagnetic field is absorbed. For simplicity we assume normal incidence, where propagation through the system does not depend on the polarization of the waves.

For a fixed oscillation frequency of the field $\omega$, the solutions to the wave equation within each layer of the medium are plane waves with spatial dependence $\exp(\pm ik_m x)$ ($m$ labels the layer). The wave vector $k_m$ is related to the frequency as $k_m = n_m \omega/c$. The electric field $\mathbf{E}$ at every point in space is thus written as a sum of two parts; namely, a *right*-moving wave $e_m^{(+)}(x) = A_m^{(+)} e^{ik_m x}$ and a *left*-moving wave $e_m^{(-)}(x) = A_m^{(-)} e^{-ik_m x}$, with the understanding that the full field is the sum of the two

  

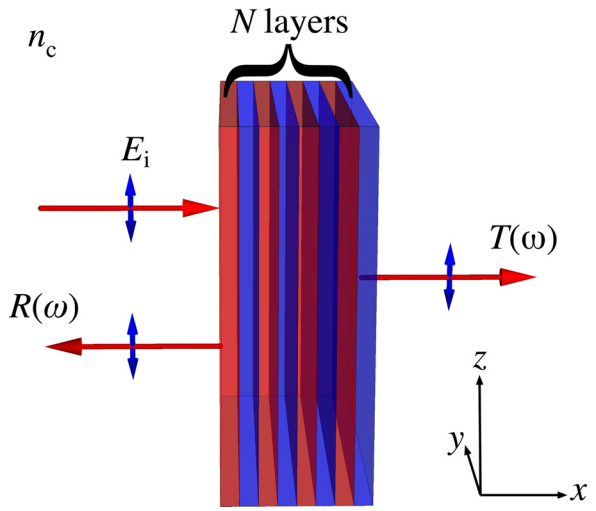


Fig. 1. An $N$-layer structure is surrounded by a medium with a real refractive index $n_c$. Linearly polarized light of frequency $\omega$ is incident from the left with electric field amplitude $E_i$, some of which is reflected with reflectivity $R(\omega)$, and some of which is transmitted with transmissivity $T(\omega)$.

$$\mathbf{E}(x) = \hat{\mathbf{p}}\left[A_m^{(+)}e^{ik_m x} + A_m^{(-)}e^{-ik_m x}\right]. \tag{1}$$

Here, $\hat{\mathbf{p}}$ is a unit vector denoting the polarization of the waves and $x$ is a position within the $m$th layer. If we introduce the column vectors $\mathbf{e}_m(x)$, the elements of which are $e_m^{(+)}(x)$ and $e_m^{(-)}(x)$, a $2\times 2$ matrix $\mathbf{M}$—the *transfer* matrix—can be found to relate the field $\mathbf{E}$ on either side of the multilayered medium. The relationship between the electric field on either side of an $N$ layered medium, such as that illustrated in Fig. 1, is $\mathbf{e}_{N+1} = \mathbf{M}\cdot\mathbf{e}_0$.

There are only two eventualities for light during propagation through a layered medium. It can encounter a boundary or continue moving through a homogeneous region. The matrix $\mathbf{M}$ can thus be broken into a product of component transfer matrices, each of which is either an *interface* matrix $\mathbf{W}$, giving the relation between the electric field on each side of a boundary, or a *translation* matrix $\mathbf{X}$, giving the relationship between the electric field on each side of a homogeneous region.

The interface matrix $\mathbf{W}$ is found by applying the condition of continuity of the relevant components of the electromagnetic field across a boundary.[14] Assuming normal incidence onto a boundary between index $n_a$ and $n_b$, these conditions are that the field and its first derivative are continuous, so that

$$e_a^{(+)} + e_a^{(-)} = e_b^{(+)} + e_b^{(-)} \tag{2}$$

and

$$n_a\left[e_a^{(+)} - e_a^{(-)}\right] = n_b\left[e_b^{(+)} - e_b^{(-)}\right], \tag{3}$$

where we have used the relation $\partial e_a^{(\pm)}/\partial x = \pm ik_a e_a^{(\pm)}$. In matrix form, Eqs. (2) and (3) can be written

$$\begin{pmatrix} e_b^{(+)} \\ e_b^{(-)} \end{pmatrix} = \frac{1}{2}\begin{pmatrix} 1+n_a/n_b & 1-n_a/n_b \\ 1-n_a/n_b & 1+n_a/n_b \end{pmatrix}\begin{pmatrix} e_a^{(+)} \\ e_a^{(-)} \end{pmatrix}. \tag{4}$$

The matrix (including the factor of 1/2) on the right of Eq. (4) is the interface matrix $\mathbf{W}^{(ab)}$, which gives the relation between the electric field across a boundary between a region of index $n_a$ and one of $n_b$.

The translation matrix $\mathbf{X}$ between two points ($x_1$ and $x_2$) in a homogeneous medium multiplies $e^{(+)}$ and $e^{(-)}$ by a phase factor $\exp[\pm ik_x(x_2 - x_1)]$. For example, for a medium of index $n_a$, we have

$$\begin{pmatrix} e_a^{(+)}(x_2) \\ e_a^{(-)}(x_2) \end{pmatrix} = \begin{pmatrix} e^{ik_a(x_2-x_1)} & 0 \\ 0 & e^{-ik_a(x_2-x_1)} \end{pmatrix}\begin{pmatrix} e_a^{(+)}(x_1) \\ e_a^{(-)}(x_1) \end{pmatrix}. \tag{5}$$

The matrix to the right of the equality in Eq. (4) is the translation matrix $\mathbf{X}^{(a)}(x_2 - x_1)$. The two matrices within Eqs. (4) and (5) can be used to study light propagation in *generic* stratified media and, as a limiting case, continuously inhomogeneous media.[5]

## III. THE BRAGG REFLECTOR

The Bragg reflector is a stratified medium composed of a periodic sequence of identical unit cells[13,15] Here the unit cell consists of two layers, each having different complex refractive indices ($n_a$ and $n_b$) and thicknesses ($a$ and $b$). Following Sec. II, we look to find the transfer matrix associated with light passing through a Bragg reflector, as illustrated in Fig. 1. The field on either side of a single unit cell is related by a matrix $\mathcal{M}_1$ that is given in terms of the interface and translation matrices associated with the individual layers in the unit cell,

$$\mathcal{M}_1 = \mathbf{W}^{(ba)}\cdot\mathbf{X}^{(b)}(b)\cdot\mathbf{W}^{(ab)}\cdot\mathbf{X}^{(a)}(a) = \begin{pmatrix} [\cos(k_b b) + i\alpha_{ab}\sin(k_b b)]e^{ik_a a} & -i\beta_{ab}\sin(k_b b)e^{-ik_a a} \\ i\beta_{ab}\sin(k_b b)e^{ik_a a} & [\cos(k_b b) - i\alpha_{ab}\sin(k_b b)]e^{-ik_a a} \end{pmatrix}, \tag{6}$$

where $k_{a,b} = n_{a,b}\,\omega/c$, $\alpha_{ab} = (n_a^2 + n_b^2)/(2n_a n_b)$ and $\beta_{ab} = (n_a^2 - n_b^2)/(2n_a n_b)$.

The transfer matrix associated with $N$ (identical) unit cells is then given by $\mathcal{M}_N = (\mathcal{M}_1)^N$. Now, there is a general result that the $N$th power of a $2\times 2$ matrix can be written in terms of Chebyshev polynomials of the second kind $U_N(z)$,[1,5,6] so that

$$\mathcal{M}_N = (\mathcal{M}_1)^N = U_{N-1}(z)\mathcal{M}_1 - U_{N-2}(z)\mathbb{1}_2, \tag{7}$$

where

$$z = \frac{1}{2}\mathrm{Tr}(\mathcal{M}_1) = \cos(k_b b)\cos(k_a a) - \alpha_{ba}\sin(k_b b)\sin(k_a a). \tag{8}$$

To compute these Chebyshev polynomials, it is usually best to use their relation to trigonometric functions[16] given by $U_N(z) = \sin[(N+1)\arccos(z)]/\sqrt{1-z^2}$.

The final expression for the complete transfer matrix $\mathbf{M}$ for the situation illustrated in Fig. 1 is when $\mathcal{M}_N$ is placed between matrices associated with light passing from the surrounding medium (index $n_c$) into the reflector and then out again, or

$$\mathbf{M} = \begin{pmatrix} m_{11} & m_{12} \\ m_{21} & m_{22} \end{pmatrix} = \mathbf{W}^{(ac)} \cdot \mathcal{M}_N \cdot \mathbf{W}^{(ca)}. \tag{9}$$

Combining Eqs. (4), (6), and (7) to evaluate Eq. (9), one obtains the final result for the elements of the transfer matrix,

$$m_{11} = U_{N-1}(z)[z + i\alpha_{ac}\xi - i\beta_{ac}\beta_{ab}\cos(k_a a)\sin(k_b b)] - U_{N-2}(z), \tag{10}$$

$$m_{12} = -U_{N-1}(z)[\beta_{ab}\sin(k_b b)(\sin(k_a a) + i\alpha_{ac}\cos(k_a a)) - i\beta_{ac}\xi], \tag{11}$$

$$m_{21} = -U_{N-1}(z)[\beta_{ab}\sin(k_b b)(\sin(k_a a) - i\alpha_{ac}\cos(k_a a)) + i\beta_{ac}\xi], \tag{12}$$

$$m_{22} = U_{N-1}(z)[z - i\alpha_{ac}\xi + i\beta_{ac}\beta_{ab}\cos(k_a a)\sin(k_b b)] - U_{N-2}(z), \tag{13}$$

where we have introduced the quantity

$$\xi = \sin(k_a a)\cos(k_b b) + \alpha_{ba}\cos(k_a a)\sin(k_b b). \tag{14}$$

The results given in Eqs. (10)–(13) immediately allow us to find the reflection and transmission coefficients of the medium. For example, when light of amplitude $E_0$ is incident from the left, the transfer matrix equation reduces to

$$\begin{pmatrix} E_0 t_+ \\ 0 \end{pmatrix} = \begin{pmatrix} m_{11} & m_{12} \\ m_{21} & m_{22} \end{pmatrix} \begin{pmatrix} E_0 \\ E_0 r_+ \end{pmatrix}, \tag{15}$$

where $r_+$ and $t_+$ are the reflection and transmission coefficients for light incident from the left-hand side of the medium. Equation (15) leads to expressions for the reflectivity and transmissivity in terms of the elements of the transfer matrix, given by

$$R_+ = |r_+|^2 = \left|\frac{m_{21}}{m_{22}}\right|^2 \tag{16}$$

and

$$T_+ = |t_+|^2 = \left|\frac{1}{m_{22}}\right|^2. \tag{17}$$

Performing the same calculation for light incident from the right, we find that $T_- = T_+$ (the determinant of $\mathbf{M}$ equals unity) and

$$R_- = |r_-|^2 = \left|\frac{m_{12}}{m_{22}}\right|^2, \tag{18}$$

which does not equal $R_+$ unless the medium is lossless, in which case Eqs. (10)–(13) show that $m_{12} = m_{21}^*$. In general $R_+$ and $R_-$ will not be equal. For example, consider a highly reflective surface backed by a thick layer of absorbing material. Light incident onto the front surface yields a reflectivity close to unity, while incidence onto the opposite side would yield a lower value. In the case of many thin layers and small dissipation, this difference is negligible and we shall often assume that $R_+ \approx R_-$. The value for $R_+$ obtained from Eq. (16) is plotted in Fig. 2, for 10 unit cells.

### A. Bloch's theorem in optics

A Bragg reflector may have tens or hundreds of layers. Nevertheless, Bloch's theorem, which strictly applies only to a system of infinite size, can be used to accurately predict the region of high reflectivity in Fig. 2. An intuitive justification for its applicability is that for frequencies where the reflectivity is high, the wave is rapidly extinguished from the medium so that the field amplitude is very close to zero at the exit interface. Thus, we can consider the number of unit cells to be infinite with little error.

If one compares an eigenmode of the field at two points in an infinite system with spatial periodicity $a + b$, the difference can only be a phase factor

$$\mathbf{E}(x + a + b) = \mathbf{E}(x)e^{i\kappa(a+b)}. \tag{19}$$

The quantity $\kappa$ is known as the Bloch wave vector and is the analogue of the free-space wave vector for the case of a discrete translational symmetry. This quantity tells us the large scale variation of the field as one moves across one or more unit cells. In terms of the transfer matrix formalism outlined in the previous two sections, the above statement is

$$\mathcal{M}_1 \cdot \mathbf{e} = e^{i\kappa(a+b)}\mathbf{e}. \tag{20}$$

Finding $\kappa$ thus amounts to finding the eigenvalues $\lambda = e^{i\kappa(a+b)}$ of the unit cell matrix $\mathcal{M}_1$ via

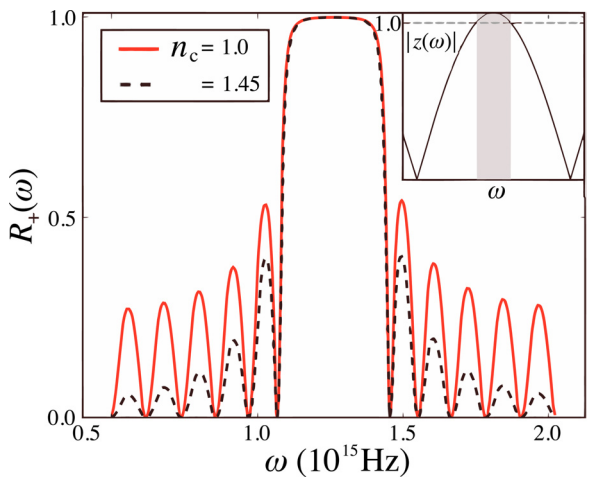


Fig. 2. Reflectivity $R_+(\omega)$ as a function of frequency for a transparent Bragg reflector composed of 10 unit cells of index $n_a = 1.45$ and $n_b = 2.1$ and thicknesses $a = 2.60 \times 10^{-7}$ m and $b = 1.76 \times 10^{-7}$ m. There is a frequency range where propagation is forbidden, corresponding to the central plateau of $R_+$, or the shaded region where $|z| > 1$ (inset). The amplitude of the oscillations increases with the index contrast of the surrounding medium $n_c$, but this does not affect the location of the plateau. *Inset*: For an infinite array of unit cells, no mode can propagate in the frequency range shaded in grey for $|z| > 1$; this is known as the photonic band gap, or stop band.

$$\det(\mathcal{M}_1 - \lambda \mathbb{1}_2) = \begin{vmatrix} \mathcal{M}_{11} - \lambda & \mathcal{M}_{12} \\ \mathcal{M}_{21} & \mathcal{M}_{22} - \lambda \end{vmatrix} = 0. \tag{21}$$

Equation (21) has the two solutions

$$\lambda = z \pm \sqrt{z^2 - 1} = e^{i\kappa(a+b)}, \tag{22}$$

where we have applied $\det[\mathcal{M}_1] = 1$, and $z = \mathrm{Tr}[\mathcal{M}_1]/2$. It can be seen directly from Eq. (8) that $z$ is real for media with real refractive indices $n_a$ and $n_b$. In this case, the criterion for allowed propagation through the multilayer becomes quite simple. When $z \leq 1$, we have

$$e^{i\kappa(a+b)} = z \pm i\sqrt{1 - z^2}, \tag{23}$$

which can be satisfied with a real Bloch wave vector $\kappa = \pm \arccos(z)/(a+b)$. Meanwhile, when $|z| > 1$ the right-hand-side of Eq. (22) is real, with one root greater and one less than unity, leading to a complex value of $\kappa$. Such solutions diverge at infinity and are therefore not allowed modes of the truly infinite system. It is in these regions of $|z| > 1$ that the system exhibits the *stop-band* shown in Fig. 2.

In a *dissipative* periodic medium (the dissipation being proportional to $1 - R_\pm - T_\pm$), the situation becomes more intricate as $z$ is now complex. To see how this modifies the situation, consider the case where a small degree of dissipation is present in an otherwise allowed frequency band. We write $z = \cos(\varphi) + i\eta$, where both $\varphi$ and $\eta$ ($\ll 1$) are real, and then expand Eq. (22) to first order in $\eta$ to get

$$e^{i\kappa(a+b)} \approx \left(1 \pm \frac{\eta}{\sin(\varphi)}\right) e^{\pm i\varphi}. \tag{24}$$

Dissipation evidently shifts the modulus of Eq. (24) away from unity. Therefore, $\kappa$ is generally complex when dissipation is present, even for modes falling within an otherwise allowed band of frequency. The distinction between allowed and forbidden bands thus becomes blurred (see Sec. IV A). This has the simple interpretation that in an absorbing periodic medium, the propagation is always damped. For large degrees of dissipation, the band-gap may even disappear.

## IV. SOME INSTANCES OF THE BRAGG REFLECTOR IN MODERN OPTICS

The above treatment of the Bragg reflector is intended to be introductory, and in nearly all respects the formulae are well known. We shall now demonstrate how these results may be used to discuss aspects of physics that are relevant to some contemporary experimental setups.

### A. An atomic Bragg mirror

A neutral atom subject to an external electric field will develop an electric dipole moment **d**. The atom will then be subject to a force due to interaction of the electromagnetic field with this induced polarization, and this force can be used to trap atoms within a confined region of space.[17] An interference pattern created by two counter-propagating laser fields creates an array of many thousands of such traps, often termed an *optical lattice*.[9]

The optical lattice is useful as a model system, but it also has interesting optical properties of its own.[18,19] We can treat this system using the formalism developed in the previous sections. In the case of a one dimensional optical lattice, where the atomic motion is only weakly constrained in the $yz$-plane, the system is essentially a slightly unusual Bragg reflector—an "atomic Bragg mirror." The reflector is approximately composed of layers of atomic clouds (width $a$, index $n_a$) and layers of vacuum (width $b$, and $n_{b,c} \approx 1$).

The expression for the index of the atomic clouds can be motivated as follows. So long as the incident electric field $\boldsymbol{E}$ is weak, the atom responds linearly and an oscillating electric dipole moment develops. Approximating this dipole moment as a simple harmonic motion of natural frequency $\omega_0$ leads to $\mathbf{d}(\omega) \propto \mathbf{E}(\mathbf{x}_0)/(\omega_0^2 - \omega^2 - i\omega\gamma)$, where $\omega$ is the frequency of the applied electric field, $\mathbf{x}_0$ is the position of the atom of interest, and $\gamma$ represents the damping of the motion. For a cloud of such atoms, the average dipole moment per unit volume $\mathbf{P} = \chi(\omega)\mathbf{E}$ must have the same $\omega$ dependence as a single dipole so that $\chi(\omega) \propto 1/(\omega_0^2 - \omega^2 - i\omega\gamma)$. Close to an atomic resonance ($\omega \approx \omega_0$) the denominator of $\chi$ can be expanded to first order in $\omega - \omega_0$ with little error, and since the susceptibility $\chi(\omega)$ is related to the refractive index[14] through the formula $n = \sqrt{(1 + \chi/\epsilon_0)}$, the index of the atomic clouds thus takes the form

$$n_a(\omega) \approx \sqrt{1 + \frac{3\pi\mathcal{N}}{(\omega_0 - \omega)/\gamma_e - i\zeta}} = \sqrt{1 + \frac{3\pi\mathcal{N}}{\delta - i\zeta}}. \tag{25}$$

In this expression, the proportionality constant and the damping have been given values that come from a more rigorous quantum mechanical analysis.[20] The quantity $\gamma_e$ is the decay rate of the excited state, and $\zeta$ is chosen to fit the width of the atomic resonance to an experimentally measured value. Finally, $\mathcal{N} = A/(k_0^3 V)$ is the number of atoms that fit into the volume $1/k_0^3$, where $k_0 = \omega_0/c$ and there are $A/V$ atoms per unit volume. For the purposes of plotting, we have defined the quantity, $\delta = (\omega_0 - \omega)/\gamma_e$, which measures how far the frequency of the incident light is from the resonant frequency of the atoms.

The main part of Fig. 3 shows the modulus of the eigenvalue defined in Eq. (22), for propagation through an infinite sequence of alternating layers of trapped atoms and vacuum. When the eigenvalue deviates from unity the wave will decay as it propagates through the medium indicating that it is not an allowed eigenmode of the infinite system, which in this case is due to a combination of both dissipation and destructive interference. The figure illustrates both this interplay between dissipation and forbidden regions of propagation ($-250 < \delta < 0$), and the remarkable fact that a stop band can exist even when the index contrast between the layers is incredibly low ($\delta > 250$). For reference, the atomic cloud index given in Eq. (25) is plotted in the two insets of Fig. 3.

Figure 4 shows reflection and transmission from a finite sequence of alternating dissipative layers. The comparative effect of introducing dissipation, but not dispersion into the system discussed in Fig. 2 is shown in Fig. 4(a), where the reflectivity is markedly reduced within the region of the stop-band as the dissipation is increased. Fig. 4(b) shows the coefficients calculated from Eqs. (17), (18), and (25), for the case of trapped $^{87}$Rb described above. We can see that when $\delta \approx 0$, where the dissipation and dispersion are both most pronounced, the optical response is quite complicated,

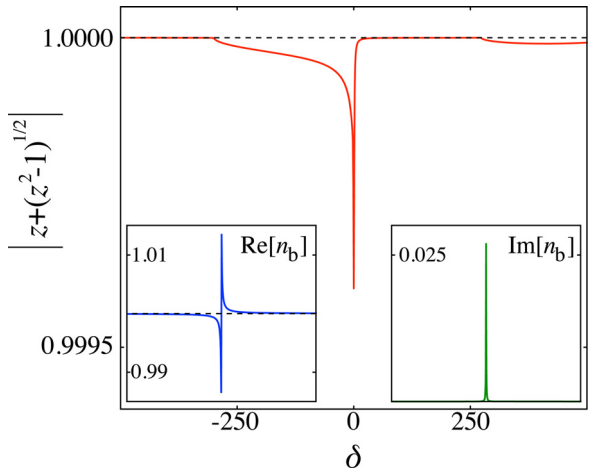


Fig. 3. The absolute value of the right hand side of Eq. (22) for a lattice of $^{87}$Rb. The deviation of this quantity away from unity indicates the magnitude of the imaginary part of the Bloch wave-vector, computed from Eq. (22). Inset: The real and imaginary parts of the refractive index given by Eq. (25) (same range of $\delta$), with $\omega_0 = 2.412 \times 10^{15}$ Hz, $\mathcal{N} = 5.7 \times 10^{-3}$, and $\gamma_e = 3.7699 \times 10^7$ Hz.

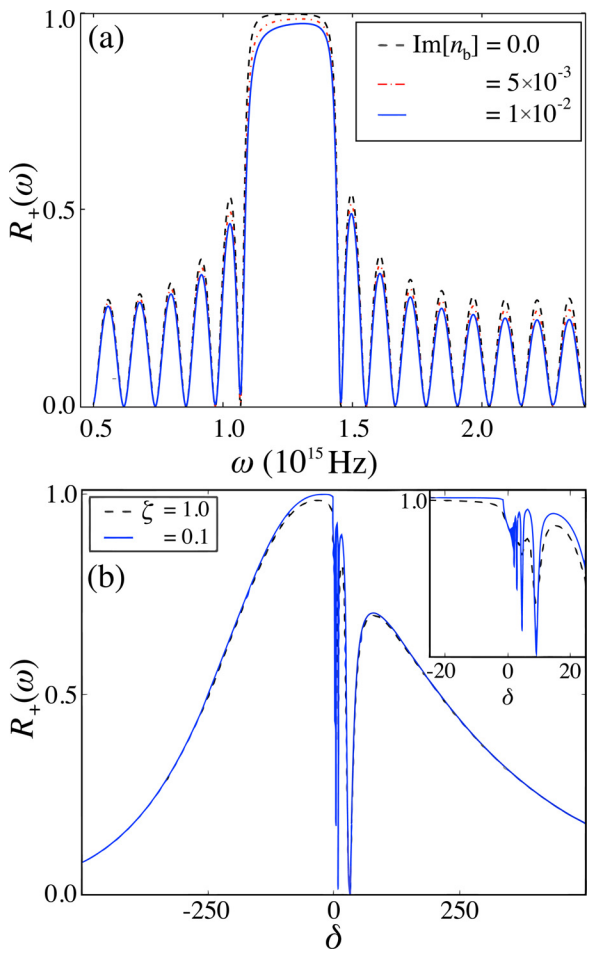


Fig. 4. Reflectivity $R_+(\omega)$ as a function of frequency for a *dissipative* Bragg reflector. (a) The dissipative analogue of the plot shown in Fig. 2; all parameters are identical but we have added an imaginary part to the refractive index $n_b$. (b) The array of unit cells now has $n_b = 1$ and $n_a$ given by Eq. (25) using the same parameter values as given in Fig. 3. The trap has $N = 5.4 \times 10^4$ periods with $a = 1.94807 \times 10^{-8}$ m, and $b = 3.70873 \times 10^{-7}$ m. The solid and dashed lines illustrate the effect of changing the line shape parameter $\zeta$.

with rapid oscillations evident on the scale of $\gamma_e$. On either side of $\delta = 0$ *two* bands of high reflectivity appear, as anticipated in Fig. 3. For $\delta < 0$, where Fig. 4(b) shows nearly total reflection, the Bloch wave vector has a significant imaginary part even though the absorption is mostly small (inset of Fig. 3). There is also a stop band evident at around $\delta \approx 250$. This is not completely shown in Fig. 4(b), where the reflectivity peaks at $\approx$0.6 for $\delta \approx 150$, but does become conspicuous for larger values of $N$.

This example system illustrates that when composed of resonant elements exhibiting significant dispersion and dissipation, the properties of the Bragg reflector can be quite subtle, and not at all like the textbook examples. Furthermore, we see that even when the layers have an index contrast of less than a percent away from unity, it is still possible to create an almost perfect reflector, so long as one can make the number of periods of the reflector large enough, which is quite possible with an optical lattice.[21,22]

### B. Optomechanical cooling

In much the same way, that atomic motion can be cooled within an optical lattice, macroscopic mechanical motion can be reduced to the point where it enters a regime where a quantum mechanical description must be used.[10,23] For example, in the case of a mechanical oscillator of frequency $\Omega$, this would be when the total energy in the center-of-mass motion becomes comparable with $\hbar\Omega$. Recent experimental work has succeeded in entering this regime[24] using a process known as optomechanical cooling. It is worth emphasizing that this cooling refers to the macroscopic oscillatory motion and not the bulk temperature of the medium. Inspired by the fact that a similar set-up has been recently proposed for this purpose,[19,25] we consider the model system illustrated in Fig. 5 to demonstrate a basic example of how the electromagnetic field may be used to reduce the kinetic energy of a moving body.

If monochromatic radiation reflects from a surface it will exert a force. For a single photon incident from the left (+) or right (–) with momentum $\pm\hbar k_\pm \hat{\mathbf{x}}$ and energy $\hbar\omega_\pm$, the difference in *optical* energy ($E^F$) before and after interaction with a planar medium is on average the difference between the intensity of outgoing and incoming waves

$$\Delta E^F_\pm = \hbar\omega_\pm [T_\pm(\omega_\pm) + R_\pm(\omega_\pm) - 1], \tag{26}$$

and the difference in optical momentum ($\mathbf{p}^F$) equals the change in the difference between the intensity of right and left going waves

$$\Delta \mathbf{p}^F_\pm = \pm\hbar k_\pm [T_\pm(\omega_\pm) - R_\pm(\omega_\pm) - 1]\hat{\mathbf{x}}. \tag{27}$$

The rate of energy and momentum being lost from the field can be equated to that taken up by the body [i.e., the negatives of Eq. (26) and (27)]. For $\mathcal{P}_\pm$ photons per second incident from the left and right, the rest-frame force on the body is minus the total momentum lost from the field (a prime denoting the rest-frame),

$$\frac{d\mathbf{p}'_{\mathrm{EM}}}{dt} = \hbar\{\mathcal{P}_+ k_+ [1 + R(\omega_+) - T(\omega_+)] - \mathcal{P}_- k_- [1 + R(\omega_-) - T(\omega_-)]\}\hat{\mathbf{x}}, \tag{28}$$

and the energy transfer to the body (bulk heating) is, similarly,

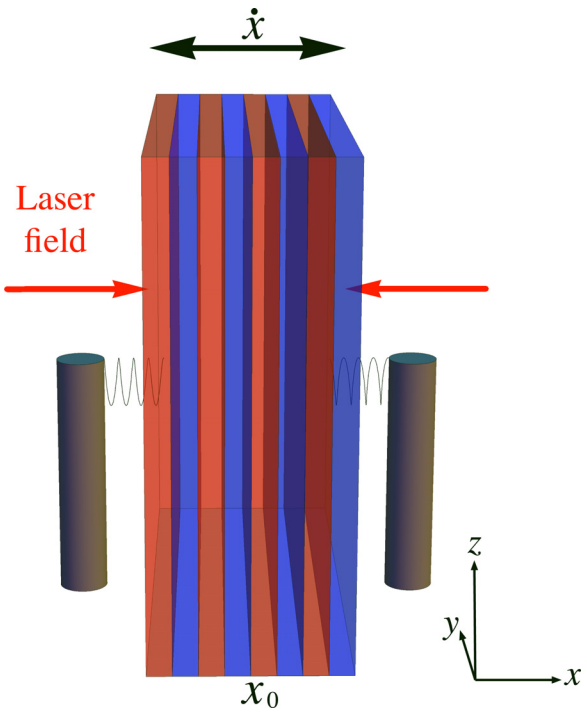


Fig. 5. A Bragg reflector confined by a pair of springs attached to fixed columns performs oscillatory motion around the point $x = x_0$. When equal-amplitude, monochromatic light is incident onto both sides of the reflector, radiation pressure can be used to add or remove kinetic energy from the motion.

$$\frac{dE'_{\rm EM}}{dt} = \hbar\{\mathcal{P}_+\omega_+[1 - R(\omega_+) - T(\omega_+)] + \mathcal{P}_-\omega_-[1 - R(\omega_-) - T(\omega_-)]\}, \tag{29}$$

where we assume that $R_+ \approx R_- = R$ and $T_+ = T_- = T$.

In the laboratory, the body is in motion with velocity $\dot{x}$ and we have monochromatic radiation of equal-amplitude $\mathcal{P}_0$ and frequency $\omega$ incident from both directions. To first order in the velocity, the rest-frame and laboratory quantities are related by a Doppler shift $\omega_\pm = \omega(1 \mp \dot{x}/c) = ck_\pm$ and $\mathcal{P}_\pm = \mathcal{P}_0(1 \mp \dot{x}/c)$. In terms of laboratory frame quantities, the force given by Eq. (28) is proportional to the velocity of the body

$$\frac{d\mathbf{p}'_{\rm EM}}{dt} = -\frac{2\hbar\omega\mathcal{P}_0}{c}\left(\frac{\dot{x}}{c}\right)\left\{\omega\left[\frac{\partial R(\omega)}{\partial\omega} - \frac{\partial T(\omega)}{\partial\omega}\right] + 2[1 + R(\omega) - T(\omega)]\right\}\hat{\mathbf{x}}, \tag{30}$$

while the energy transfer given by Eq. (29) is independent of the velocity,

$$\frac{dE'_{\rm EM}}{dt} = 2\hbar\omega\mathcal{P}_0[1 - R(\omega) - T(\omega)]. \tag{31}$$

Here, the reflection and transmission coefficients have been expanded to first order as a Taylor series around the laboratory frequency $\omega$, giving $R(\omega_\pm) \approx R(\omega) \mp (\dot{x}\omega/c)\partial R(\omega)/\partial\omega$ and a similar expression for $T(\omega_\pm)$. Finally, we transform Eqs. (28) and (29) into the laboratory frame to find the observed mechanical force on the body, which is a combination of both the rest-frame force Eq. (30) and energy transfer Eq. (31). This force is $d\mathbf{p}_{\rm EM}/dt \approx d\mathbf{p}'_{\rm EM}/dt + (\dot{\mathbf{x}}/c^2)dE'_{\rm EM}/dt$, which we find to be

$$\frac{d\mathbf{p}_{\rm EM}}{dt} = -\frac{2\hbar\omega\mathcal{P}_0}{c}\left(\frac{\dot{x}}{c}\right)\left\{1 + 3R(\omega) - T(\omega) + \omega\left[\frac{\partial R(\omega)}{\partial\omega} - \frac{\partial T(\omega)}{\partial\omega}\right]\right\}\hat{\mathbf{x}}. \tag{32}$$

Equation (32) gives the optical contribution to the force on the moving reflector illustrated in Fig. 5. Defining the damping coefficient $\Gamma$ by

$$\Gamma = \frac{\hbar\omega\mathcal{P}_0}{c^2}\left\{1 + 3R(\omega) - T(\omega) + \omega\left[\frac{\partial R(\omega)}{\partial\omega} - \frac{\partial T(\omega)}{\partial\omega}\right]\right\}, \tag{33}$$

the equation of motion for the center-of-mass for this system takes the familiar form

$$m\frac{d^2x}{dt^2} + 2\Gamma\frac{dx}{dt} + m\Omega^2(x - x_0) = 0, \tag{34}$$

where $m$ is the mass of the reflector and $\Omega$ is the frequency associated with the restoring force of the springs. Equation (34) is that of a damped ($\Gamma > 0$) or amplified ($\Gamma < 0$) harmonic oscillator. The damping coefficient is proportional to the incident optical power, and depends on the reflection and transmission coefficients and their derivatives with respect to frequency. The solutions to Eq. (34) are

$$x(t) = x_0 + A_0 e^{-\Gamma t/m} e^{\pm i\Omega\sqrt{1 - \Gamma^2/m^2\Omega^2}\,t}, \tag{35}$$

where $A_0$ is the distance of the center-of-mass from $x_0$ at $t = 0$. If the medium is only weakly dispersive, then the derivatives of the reflection and transmission coefficients within Eq. (33) may be neglected, and $\Gamma$ is then positive. It is then clear that the rate of damping is ordinarily very small. For instance, an optical field with $\omega \approx 10^{15}$ Hz and a very small mass[25] $m \approx 10^{-15}$ kg yields $\Gamma/m \approx 10^{-21}\mathcal{P}_0$. To obtain moderate damping, say $\Gamma/m \approx 10^{-3}$, would thus require an incident power of $\hbar\omega\mathcal{P}_0 \approx 10^{-1}$ W. In such a field the heating due to absorption alone would be enough to destroy such a small body.

Conversely, for a Bragg reflector dispersion is not negligible. Figure 2 shows that there are strong oscillations in the reflection and transmission coefficients, contributing significantly to $\Gamma$ via the frequency derivatives in Eq. (33). The motion can then be either amplified (heated) or damped (cooled), depending on the sign of the derivatives of the reflection and transmission coefficients. For a rapidly increasing reflectivity with frequency we have damping ($\Gamma > 0$), while for a rapidly decreasing reflectivity with frequency we have amplification ($\Gamma < 0$). Figure 6 shows a plot of $c^2\Gamma/\hbar\omega\mathcal{P}_0$, demonstrating four orders of magnitude increase in the absolute value of the damping coefficient. The required optical power density is correspondingly four orders of magnitude smaller. The above effect presents a basic example of optomechanical cooling.

### C. Optical nonreciprocity

Reciprocity, or the fact that a detector will show the same reading when the positions of a source and detector of waves

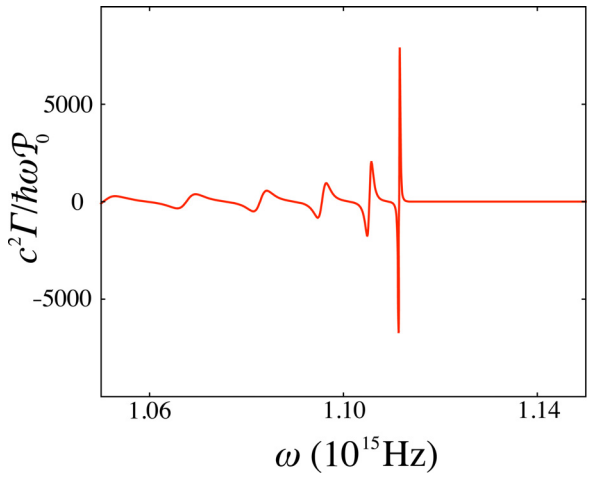


Fig. 6. The damping coefficient of the motion $\Gamma$ (in units of $\hbar\omega\mathcal{P}_0/c^2$) for a Bragg reflector at a frequency around the edge of a stop band. The parameters are the same as in Fig. 2 but for $N=50$ layers.

are interchanged, is a rather general property of wave propagation. Yet for the purposes of performing signal processing one might like to realize an "optical diode," allowing total light transmission in the forward direction while inhibiting (over some bandwidth) propagation in the backward direction. A moving Bragg reflector provides a simple example of a system exhibiting significant nonreciprocity (due to the motion, which breaks time symmetry), and close to the stop-band edge its properties can be much like that of an optical diode.

If a medium is reciprocal, then the transmission from the background index on the left of the medium to that on the right should be the same as transmission from right to left. We define here a simple measure of the nonreciprocity of our layered medium to be

$$\Delta T = T_+(\omega) - T_-(\omega), \tag{36}$$

where the transmission coefficients are those measured in the laboratory with source and detector on opposite sides of the $N$-layered medium shown in Fig. 1. This measure does not capture everything that the full definition of reciprocity captures,[14] but it should agree qualitatively. Computing $T_+$ and $T_-$ as in Eq. (17), one obtains $T_+ = |\det(\mathbf{M})/m_{22}|^2$ and $T_- = |1/m_{22}|^2$, so that for $T_+$ to equal $T_-$ we must have $\det[\mathbf{M}] = 1$. For normal incidence, an arbitrary transfer matrix is equal to a product of the $\mathbf{X}$ and $\mathbf{W}$ matrices given by Eqs. (4) and (5). The determinant of such a product equals the product of the determinants, or

$$\begin{aligned}\det[\mathbf{M}] &= \prod_{i=1}^{N}\det[\mathbf{X}^{(i)}(d_i)]\prod_{j=0}^{N}\det[\mathbf{W}^{(j,j+1)}]\\ &= \prod_{j=0}^{N}\frac{n_j}{n_{j+1}} = \frac{n_0}{n_{N+1}} = 1,\end{aligned} \tag{37}$$

where we have assumed an $N$-layered medium, each layer having index $n_i$ and thickness $d_i$. In the case where source and detector reside in different media ($n_0 \neq n_{N+1}$), this simple measure must be modified.

Reciprocity is therefore unavoidably embedded within the $2\times 2$ transfer matrix formalism. To break reciprocity the formalism must be broken. Perhaps the simplest way to do this is to take a medium that has been set into motion. Then we cannot take $\omega$ to be the same throughout the system. Reflection causes the frequency of the waves to become $\omega_\pm = \omega(1\mp\dot{x}/c)$ and this will depend on the direction of incidence. Therefore, incident left- and right-going waves of frequency $\omega$ will generate reflected and transmitted waves of frequencies $\omega_\pm$ and $\omega$. In effect, for two input channels we have four output channels.

To calculate Eq. (36) for our system, consider the electric field in the rest-frame. For incidence from the left, the rest-frame field on either side of the medium is

$$\mathbf{E}'(x') = \begin{cases} E_+\,\hat{\mathbf{z}}\left[e^{i\omega_+ x'/c} + r_+(\omega_+)e^{-i\omega_+ x'/c}\right] & x' < 0\\ E_+\,\hat{\mathbf{z}}\,t(\omega_+)e^{i\omega_+ x'/c} & x' > L,\end{cases} \tag{38}$$

and for incidence from the right

$$\mathbf{E}'(x') = \begin{cases} E_-\,\hat{\mathbf{z}}\,t(\omega_-)e^{-i\omega_- x'/c} & x' < 0\\ E_-\,\hat{\mathbf{z}}\left[e^{-i\omega_- x'/c} + r_-(\omega_-)e^{i\omega_- x'/c}\right] & x' > L,\end{cases} \tag{39}$$

where the medium is taken to be of length $L$. Equations (38) and (39) are transformed into the laboratory frame using the first-order transformation $\mathbf{E} = \mathbf{E}' - \dot{\mathbf{x}}\times\mathbf{B}'$. Having done this, the transmitted electric field is simply modified by a change in the field amplitude and a Doppler-shifted frequency appearing within the argument of the rest-frame transmission coefficient,

$$\mathbf{E}(x) = \begin{cases} E_0\,\hat{\mathbf{z}}\,t(\omega_+)e^{i\omega x/c} & x > L + \dot{x}t \quad \text{(left)}\\ E_0\,\hat{\mathbf{z}}\,t(\omega_-)e^{-i\omega x/c} & x < \dot{x}t, \quad \text{(right)},\end{cases} \tag{40}$$

where $E_+ = E_0(1-\dot{x}/c)$ and $E_- = E_0(1+\dot{x}/c)$. The difference in laboratory frame transmissivities for left and right incidence can thus be inferred from Eq. (40) to be

$$\Delta T = T_+ - T_- = |t(\omega(1-\dot{x}/c))|^2 - |t(\omega(1+\dot{x}/c))|^2. \tag{41}$$

To first order in the velocity of the medium, Eq. (41) is

$$\Delta T \approx -\frac{2\omega\dot{x}}{c}\frac{\partial T(\omega)}{\partial\omega}, \tag{42}$$

where $T(\omega)$ is the rest-frame transmissivity. If dispersion is moderate, then this nonreciprocity is negligibly small for realistic velocities (if $T$ changes 0.1 over $10^{15}$ Hz, then for optical frequencies and $\dot{x}\approx 1$ m/s, $\Delta T \approx 10^{-9}$). However, when the rest-frame transmission coefficient depends strongly on frequency, then Eq. (41) may be large. We again see the Bragg reflector illustrates a prime example of this. Figure 7 shows a plot of $\Delta T$ for an atomic Bragg mirror set into motion[26] at 1 m/s and 5 m/s. Due to the strongly dispersive optical response of the lattice (Fig. 4), the non–reciprocity of this system as determined by $\Delta T$ can be in the tens of percent for velocities of meters per second.[27] For the same velocity regime, an effective optical diode would require only an order of magnitude increase in the dispersion.

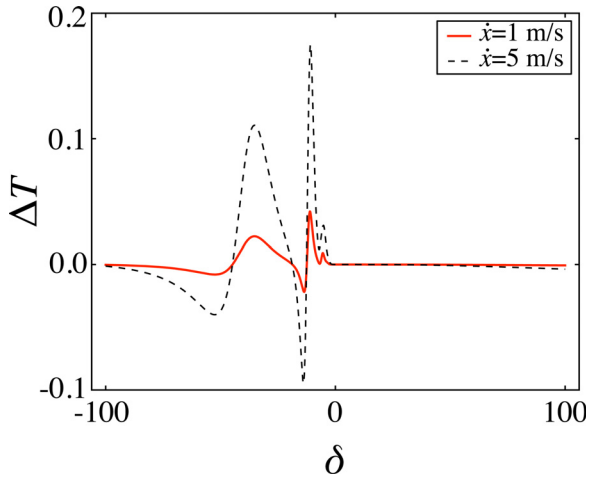


Fig. 7. Non reciprocal response, given by Eq. (36), for an atomic Bragg mirror set in motion. The velocity is 1 m/s (solid) and 5 m/s (dashed). The parameters are the same as given in Fig. 4(b).

## V. CONCLUSIONS

We have given an overview of the properties of the Bragg reflector using a simple application of the transfer matrix formalism. The basic physics of this system was found to be convenient for discussing several topical areas of optical physics. We used it as the basis for a discussion of optomechanical cooling and optical nonreciprocity effects, which can all be observed by using Bragg mirrors made of ultracold atoms.

## ACKNOWLEDGMENTS

SARH thanks the EPSRC for financial support. This work is supported by the National Natural Science Foundation of China (11104112), the National Basic Research Program of China (2011CB921603), the CRUI-British Council Programs "Atoms and Nanostructures" and "Metamaterials," the IT09L244H5 Azione Integrata MIUR Grant and the 2011 Fondo di Ateneo of Brescia University. Two of us (M.A. and G.L.R.) would like to thank J.-H. Wu for the hospitality at Jilin.

[a]Electronic mail: s.horsley@exeter.ac.uk

[1]D. J. Griffiths and C. A. Steinke, "Waves in locally periodic media," Am. J. Phys. **69**, 137–154 (2001).
[2]J. M. Ziman, *Principles of the Theory of Solids* (Cambridge U.P., Cambridge, UK, 1972).
[3]E. M. Lifshitz and L. P. Pitaevskii, *Statistical Physics (Part 2)* (Butterworth–Heinemann, Oxford, UK, 2003).
[4]R. J. Olsen and G. Vignale, "The quantum mechanics of electron conduction in crystals," Am. J. Phys. **78**, 954–960 (2010).
[5]M. Born and E. Wolf, *Principles of Optics* (Cambridge U.P., 1999).
[6]D. J. Griffiths and N. Taussig, "Scattering from a locally periodic potential," Am. J. Phys. **60**, 883–888 (1992).
[7]W. Guo, "Optical band gaps as a result of destructive superposition of scattered waves," Am. J. Phys **74**, 595–599 (2006).
[8]L. L. Sánchez–Soto, J. J. Monzòn, A. G. Barriuso and J. F. Cariñena, "The transfer matrix: A geometrical perspective," Phys. Rep. **513**, 191–227 (2012).
[9]I. Bloch, "Ultracold quantum gases in optical lattices," Nat. Phys. **1**, 23–30 (2005).
[10]F. Marquardt and S. M. Girvin, "Optomechanics," Physics **2**, 40 (2009).
[11]R. J. Potton, "Reciprocity in optics," Rep. Prog. Phys. **67**, 717–754 (2004).
[12]D. Dai, J. Bauters, and J. E. Bowers, "Passive technologies for future large–scale photonic integrated circuits on silicon: polarization handling, light non–reciprocity and loss reduction," Nature Light Sci. Appl. **1**, e1 (2012).
[13]P. Yeh, *Optical Waves in Layered Media* (Wiley, NJ, 2005).
[14]L. D. Landau, E. M. Lifshitz, and L. P. Pitaevskii, *The Electrodynamics of Continuous Media* (Butterworth–Heinemann, Oxford, UK, 2004).
[15]O. S. Heavens, "Optical properties of thin films," Rep. Prog. Phys. **23**, 1–63 (1960).
[16]I. S. Gradshteyn and I. M. Ryzhik, *Tables of Integrals, Series and Products* (Academic Press, San Diego, CA, 2000).
[17]R. Grimm, W. Weidemüller and Y. B. Ovchinnikov, "Optical dipole traps for neutral atoms," Adv. At. Mol. Opt. Phys. **42**, 95–170 (2000).
[18]M. Artoni, G. C. La Rocca, and F. Bassani, "Resonantly absorbing one–dimensional photonic crystals," Phys. Rev. E **72**, 046604 (2005).
[19]S. A. R. Horsley, M. Artoni, and G. C. La Rocca, "Radiation damping in atomic photonic crystals," Phys. Rev. Lett. **107**, 043602 (2011).
[20]J. Weiner and P.-T. Ho, *Light–Matter Interaction: Fundamentals and Applications* (Wiley–Interscience, 2003), Vol. 1.
[21]A. Schilke, C. Zimmermann, P. W. Courteille, and W. Guerin, "Photonic band gaps in one–dimensionally ordered cold atomic vapors," Phys. Rev. Lett. **106**, 223903 (2011).
[22]A. Schilke, C. Zimmermann, and W. Guerin, "Photonic properties of one-–dimensionally–ordered cold atomic vapors under conditions of electromagnetically induced transparency," Phys. Rev. A **86**, 023809 (2012).
[23]M. Aspelmeyer, S. Gröblacher, K. Hammerer, and N. Kiesel, "Quantum optomechanics—throwing a glance," J. Opt. Soc. Am. B **27**, A189–A197 (2010).
[24]J. Chan, T. P. Mayer Alegre, A. H. Safavi–Naeini, J. T. Hill, A. Krause, S. Gröblacher, M. Aspelmeyer, and O. Painter, "Laser cooling of a nanomechanical oscillator into its quantum ground state," Nature **478**, 89–92 (2011).
[25]K. Karrai, I. Favero, and C. Metzger, "Doppler optomechanics of a photonic crystal," Phys. Rev. Lett. **100**, 240801 (2008).
[26]An atomic Bragg mirror may be set into motion by relatively detuning the two trapping laser beams so that the interference pattern moves along at a velocity determined by the detuning. Alternatively the lattice may be given a sudden jolt so that the atoms slosh about within the wells. In this latter case the velocity of the medium is a periodic function of time.
[27]S. A. R. Horsley, J.-H. Wu, M. Artoni, and G. C. La Rocca, "Optical nonreciprocity of cold atom Bragg mirrors in motion," Phys. Rev. Lett. **110**, 223602 (2013).